A GLOBAL MAP OF GULLIED HILLSLOPES. A. Noblet[1] and S.J. Conway[1], [1]Laboratoire de Planétologie et Géodynamique, CNRS UMR 6112, Université de Nantes, France (axel.noblet@univ-nantes.fr).

Introduction: Gullies on Mars are geologically recent channelized landforms that share morphological characteristics with terrestrial gullies that are carved by liquid water [1]: e.g., alcove with a tributary system, sinuous channel, fan with overlapping deposits. Gullies are found on sloping terrain in both hemispheres of Mars, between roughly 30° and 80° of latitude and spanning all longitudes.

Monitoring has revealed current gully activity, with downslope movement of material [2]. The activity occurs predominantly during local winter at times of active defrosting, which suggests a process involving not liquid water but CO_2 ices. The aim of this mapping effort is to provide a complete global martian gully catalog, to constrain their formation mechanisms and to enable precise targeting by ongoing missions for monitoring purposes.

The previous mapping effort by Harrison *et al.* [3] compiled a global inventory of 4861 gullied landforms (including craters, valley sides, mesas and dunes). They did not map the extent of the gullies themselves. Some of these landforms are several (tens of) kilometers in size and host several gully clusters separated by a relatively large distance. Our mapping instead delimits the extent of gullied hillslopes for each of the sites previously mapped by [3], and for other sites we observed which were not previously identified.

Methods: We mapped the outline of the gullied area as polygons using ArcGIS for each site of [3] (Fig.1). We included the polygons from [4] which cover gullied slopes in Terra Cimmeria, Argyre and Acidalia Planitia. The basemap used is a global MRO ConTeXt Camera (CTX) [5] mosaic made available by the Murray Laboratory at the California Institute of Technology [6] at a resolution of 5.0 m/px. The mosaic covers 88°S to 88N°. Thus, the whole latitudinal range of gullies is covered. We also used georeferenced High Resolution Imaging Science Experiment (HiRISE) [7] browse products (~3 m/px) where available.

Where relevant we linked our gully-polygons to the global crater database by Robbins and Hynek [8] to obtain the percentage of gullied craters and their depth/Diameter (d/D) ratio where depth information is available (diameters > 3 km). For each crater we assess a gully occupation percentage, by dividing gullied area by an estimation of crater wall area. Finally, using the publicly available HiRISE footprint shapefile, we assess the number of HiRISE images acquired for each gully polygon to identify future targets.

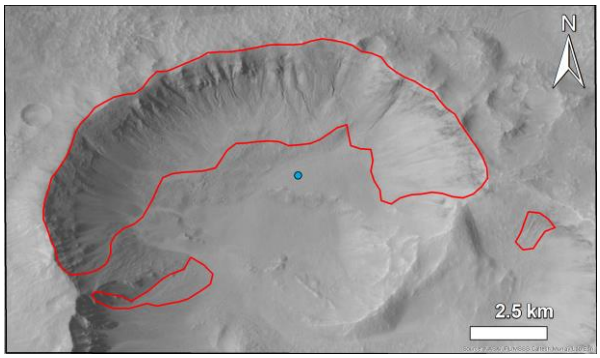

Fig. 1: representation of gullied hillslopes as polygons in red, compared to the point representation, in blue, used in previous mapping [3] - site #2369 (38.6S°, -163.3E°).

Results: We mapped 7833 gullied hillslopes, amounting to 40 630 km² of gullied area. 87% of the gullied area is located in the southern hemisphere, compared to 88% if we only consider the gullies as point-features. The scale of the mapped features varies from a single gully at $6x10^{-3}$ km² to extensive slopes covered by many tens of gullies, spanning up to nearly 110 km in length and covering up to 500 km². Out of the 187 sites previously mapped by [3] (3% of the total analyzed) we could not formally identify any gullies, due to high image noise, shaded area or missing coverage of both CTX and HiRISE.

In the latitudinal bands of gully occurrence, 1.7% of all craters contain gullies and the average gullied crater diameter is 17±20 km. 54.2% of gullied craters are larger than 6 km in diameter, which is around the simple to complex crater transition [9]. The d/D ratio of a crater can be used as a proxy for its degradation state, with a lower value corresponding to a more topographically diffuse, degraded crater. We plot the gully occupation percentage as a function of the d/D ratio of gullied craters and of non-gullied craters (Fig.2). We observe that gullied craters are in the upper range of d/D values, corresponding to fresher morphology, compared to the non-gullied craters. This trend is consistent across all latitudinal bins. For a given diameter, gullied craters with a higher d/D value tend to have a higher gully occupation percentage which is highest in craters between 35 to 50°S. We also observe that some craters with the highest d/D value are not gullied.

Our density map of gullies shows similar results to previous studies [3,4] (Fig.3), with a higher gully density in the southern hemisphere and high-density spots with as much as 31% of a square degree being covered by gullies in Argyre Planitia.

37.3% of gullied slopes (n=2922) we mapped have been imaged by HiRISE at least once and 18.8% (n=1472) have been imaged twice or more. The majority of gullied slopes lack HiRISE coverage, and hence it is important to cover these missing sites for future repeat imaging.

Discussion, conclusions and future work: Our observations show that the degradation state of a crater is an important parameter for gully development: gullies develop mostly in 'fresh' or less degraded craters, and the most developed gully clusters are found within the 'freshest' craters. This can be explained by the greater availability of steep hillslopes in fresh craters, as they are less topographically diffuse than degraded craters. We have also observed that gullies occur preferentially in complex craters, which tend to have more hillslopes than simple craters due to the presence of central peaks and terraces. Some fresh craters do not display any gullies; therefore, crater morphology cannot solely explain the distribution of gullies.

Our analysis also highlights the fact that the current catalog of active gully sites is largely under-populated, as 81.2% of all gullied slopes do not have repeated high-resolution coverage, if any. Finally, our mapping effort constitutes the most complete catalog of martian gullies to date and will enable for precise targeting and monitoring by ongoing and future missions, as well as comparison with other global datasets (e.g., albedo, thermal infrared, spectral maps…). Further work will include an analysis of density as a function of slope, a re-examination of sites where we could not identify gullied slopes with individual CTX images and slope and aspect analysis.

Acknowledgments: We acknowledge the financial support from Région Pays de la Loire, project étoiles montantes METAFLOWS (Nº 2019-14294) and the French Space Agency, CNES.

References: [1] M.C. Malin and K.S. Edgett (2000) *Science*, 288, 2330–2335. [2] C.M. Dundas et al. (2019) *Geological Society, London, Special Publications*, 467, 67–94. [3] T.N. Harrison et al. (2015) *Icarus*, 252, 236–254. [4] S.J. Conway et al. (2019) *Geological Society, London, Special Publications*, 467, 187–197. [5] M.C. Malin et al. (2007) *J. Geophys. Res.*, 112, E05S04. [6] J. L. Dickson et al. (2018) in 2. [7] A.S. McEwen et al. (2007) *J. Geophys. Res.*, 112, E05S02. [8] S.J. Robbins and B.M. Hynek (2012) *J. Geophys. Res.*, 117. [9] S.J. Robbins and B.M. Hynek (2012) *J. Geophys. Res.*, 117.

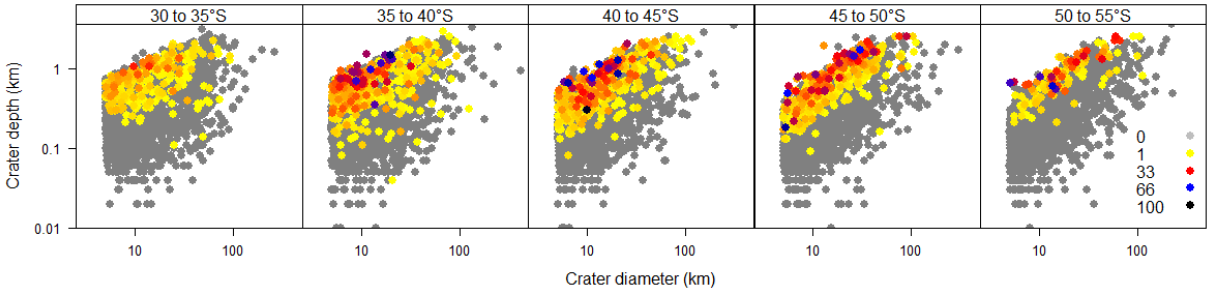

Fig. 2: Scatter plots of depth against diameter for gullied craters in the southern hemisphere within 5-degrees latitude bins. Gully occupation percentage is represented with a color scale (key in the right panel), and non-gullied craters are grey points.

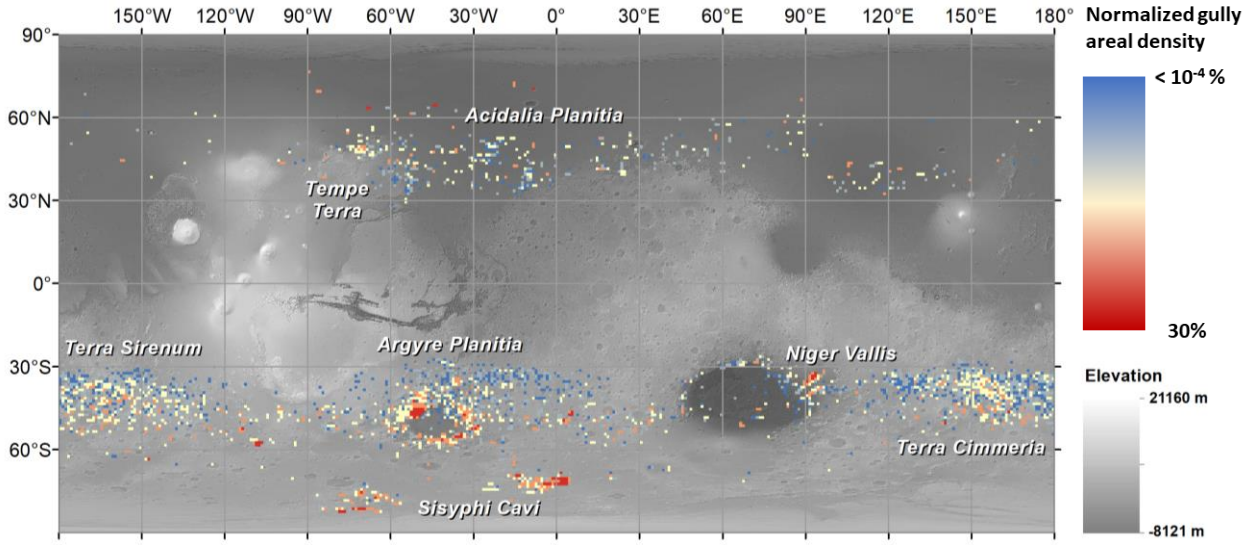

Fig. 3: Global map of normalized gully areal density per 1° square windows. Basemap is greyscale and hillshaded MOLA topography data, where whte is high elevation and darker tones low elevation.